Dynamic Beamforming Algorithms for Ultra-directional Terahertz Communication Systems Based on Graphene-based Plasmonic Nano-antenna Arrays

Michael Andrello III*, Arjun Singh†, Ngwe Thawdar* and Josep Miquel Jornet†

†Department of Electrical Engineering, University at Buffalo, The State University of New York, Buffalo, NY 14260, USA, E-mail: {asingh29, jmjornet}@buffalo.edu
*Air Force Research Laboratory, Information Directorate, Rome, NY 13441, USA, Email: {michael.andrello.1,ngwe.thawdar}@us.af.mil

***Abstract*—Terahertz-band (0.1 to 10 THz) communication is envisioned as a key wireless technology to satisfy the need for much higher wireless data rates. The use of nanomaterials such as graphene is enabling the development of miniature plasmonic devices, which intrinsically operate in the THz band. In this paper, a new antenna array architecture that leverages the properties of graphene-based plasmonic devices is presented. In the proposed architecture, each element is integrated by a THz plasmonic signal source, a THz plasmonic direct signal modulator, and a THz plasmonic nano-antenna. The very small size of the resulting frontend allows its integration in very dense arrays, which are needed to overcome the very high path-loss at THz frequencies. Moreover, new beamforming strategies at the single element level and at the integrated array level are possible. The performance of the resulting beamforming antenna arrays are derived and numerically investigated by means of electromagnetic simulations.**

I. Introduction

As next generation wireless networks face demands to support unprecedented number of connected devices and higher data rates, communications in traditionally underutilized parts of the spectrum has gained attention in research communities. To that end, terahertz band (0.1 to 10 THz) communication is envisioned as a key wireless technology to meet this demand, as THz band can provide multiple transmission windows with tens of GHz bandwidth each [1], [2]. Nevertheless, the lack of compact high power sources and highly sensitive detectors has previously hampered the full exploitation of the THz band. However, many recent advancements in materials and device technology are closing this gap. One of these advancements is the development and fabrication of novel nano-devices from nanomaterials such as graphene [3], which operate intrinsically in the THz band.

Graphene is a one atom thick layer of carbon atoms in a honey comb lattice, and possesses unique electric properties. In addition, such properties can be tuned by changing the chemical potential, or Fermi energy (i.e., by applying a variable voltage to the graphene layer). This electrical tunability of graphene can be utilized to create frequency tunable devices that can generate, modulate and transmit THz waves [4], [5]. Furthermore, graphene supports the propagation of Surface Plasmon Polariton (SPP) waves, which are highly confined EM waves at the interface of a conductor and dielectric [6], [7]. SPP waves have wavelengths that are orders of magnitude less than those of free-space EM waves at the same frequency. The highly confined wavelength of SPP waves together with the tunability of graphene allow the development of novel graphene-based communication devices.

Using the intrinsic properties of graphene and SPP waves, a graphene-based nano-transceiver is proposed as a compact efficient source for direct terahertz signal generation in [8]. The authors in [9] and [10] designed and studied a plasmonic phase modulator by exploiting the electrical tunability of graphene to modulate the SPP wave without the need of sub-harmonic mixers. In [11] and [12], the authors proposed a graphene-based nano-antenna which acts as a lossy waveguide to effectively launch SPP waves into free space. The small sizes of these nano-devices lead to low output power and a limitation on the transmission distance. To increase the overall output power of the system and to overcome the very high path loss of the THz channel, directional antenna systems such as beamforming antenna arrays are needed.

In this paper, we study the beamforming capabilities of a novel, plasmonic array architecture. For this we first present and investigate the performance of a single front end, composed of a port acting as the power source, a plasmonic modulator and the plasmonic antenna. This front end acts as the radiating element of the plasmonic array. Then the ability to beamform for a 2x2 array is shown. The array performance is compared with the performance of the single front end in terms of power output and beam directivity.

The rest of the paper is organized as follows. In Sec II, we introduce and discuss the novel plasmonic architecture. We present and expand upon the front end presented first in [13] and discuss its performance characteristics in Sec III. In Sec IV, we analyze the radiation pattern of the front end

978-1-5386-9218-9/18/$31.00 ©2018 IEEE

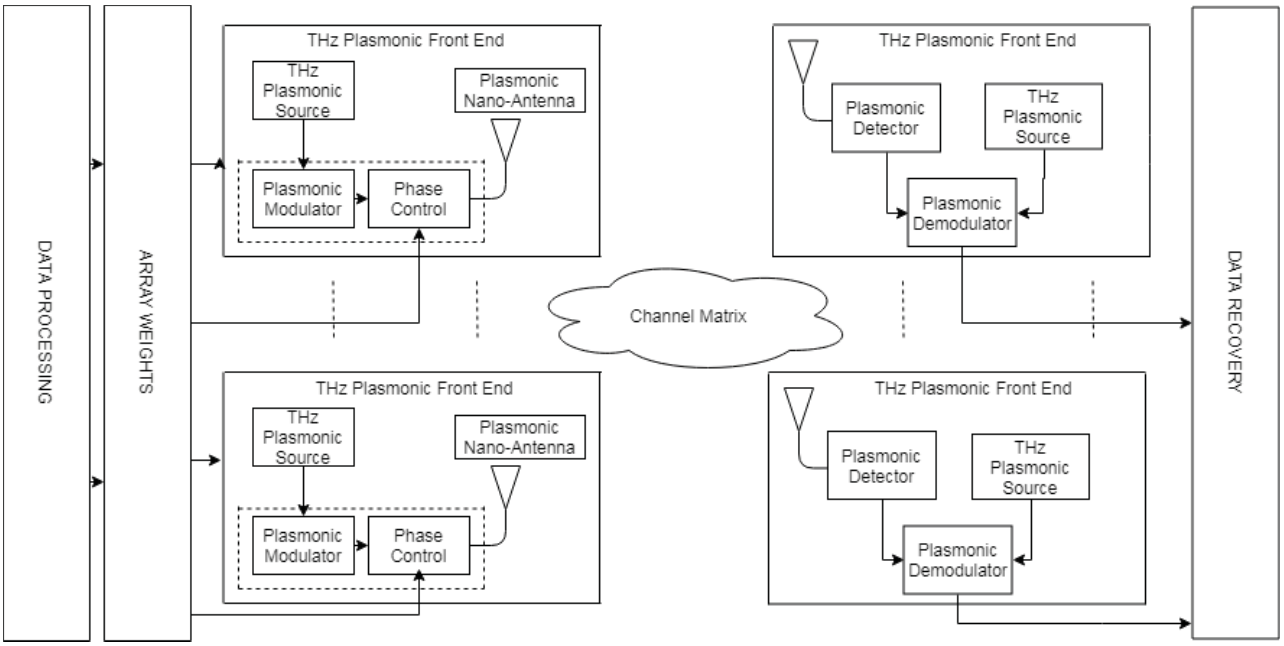

Fig. 1. System Design

in detail, and present the design of the plasmonic array. We present the results from the previous sections in Sec V. Finally, in Sec VI, we draw some conclusions and discuss the future steps to expand upon and realize this architecture.

II. System Design

A. Overview

In conventional array architectures, both digital as well as analog, the baseband signal is modulated and up-converted to the target center frequency. More specifically, in analog architecture the modulated baseband signal is up-converted and then split into N transmission lines, with its own phase controller, power amplifier and antenna. In the digital architecture, first the baseband signal is split into N transmission lines, and then phase control, power amplification and up-conversion to the target frequency is performed on each line. As the control over transmission signals is increased, the complexity of the required hardware increases. There are also several hybrid architecture schemes proposed, in which certain control is performed before up-conversion and some afterwards.

The proposed plasmonic array architecture differs from conventional array architectures in several ways. It leverages the unique plasmonic properties of the devices to greatly simplify the array design. Each radiating element of the array consists of the source, the modulator and the antenna. The plasmonic modulator can directly modulate THz frequencies without the need of sub-harmonic mixers. The nano-antenna is designed for resonance with SPP wavelength and thus is much smaller than a regular patch antenna for the same frequency. Since the mutual coupling of the radiating elements in this plasmonic array depends on SPP wavelength and not the free-space wavelength [14], these small nano-antennas can be packed into a very dense array. Thus, with a very small area footprint, the power output and beamforming capabilites of the plasmonc array can outperform a similarly designed conventional array. Also, as is discussed in detail in Sec IV, the single front end comprises of a reconfigurable radiation pattern. Thus, a single control line is also possible for all array elements, which greatly simplifies the hardware implementation. The resulting system design is shown in Fig 1.

B. Source

The plasmonic THz source is based on a High Electron Mobility Transistor fabricated with a III-V semiconductor and enhanced with graphene [15], [16]. It utilizes the Dyakanov-Shur instability principle to generate SPP waves directly in the THz range.

When the transistor source and drain are connected to the gate with correct impedances, and a DC voltage is applied, there is a resonance of electrons in the form of a 2D electron gas as per the instability principle. With the use of a graphene layer suspended on top of the gate material, SPP waves are generated which propagate towards the modulator.

C. Modulator

The modulator block is implemented to allow phase control, and was first introduced in [9]. It is designed as a layer of graphene, on top of a substrate with a ground plane beneath. The working principle of the modulator is that the velocity of the SPP waves on graphene depends on the Fermi energy of the graphene layer. Thus, for a modulator of constant length, the velocity, and in turn the phase of the SPP waves as they are

fed into the antenna, can be modified by changing the Fermi energy of the graphene layer of the modulator block [13].

The range of phase delay supported by the modulator depends on the length of the modulator, and the range of Fermi energy possible. The length of the modulator block has to be long enough to allow enough propagation space for the wavelength of the SPP waves to be delayed significantly for adequate phase change. However, a longer length will cause greater power dissipation from the source to the antenna. Thus the task presents itself as an optimization problem.

D. Antenna

The plasmonic nano-antenna is studied and developed in [13]. It acts as a lossy waveguide to eject the SPP waves into free space. Its performance and design parameters are based upon plasmonic physics which govern the propagation of SPP waves on graphene. The key factor is the conductivity of graphene, and has been discussed in detail in [13].

The plasmonic nano-antenna has to be designed for resonance with the plasmonic wavelength of the SPP waves generated in graphene, and not the free space wavelength. Since the plasmonic wavelength is much lesser than free space wavelength, the size of plasmonic antenna is much smaller than that of a regular antenna for the same resonant frequency.

III. Front End Design

In our design, the three building blocks of the plasmonic front end (source, modulator and antenna) share the same active graphene layer. As a result, the three elements need to be designed and modeled together. This section discusses the design and performance of the plasmonic front end at 1.03 THz, which is the first window above 1 THz, thus making our design work at true THz frequencies.

COMSOL multiphysics, which is a finite element numerical solver, was used as the simulation platform for these analyses. Since the plasmonic source is based upon a hydro-dynamic model for electron transport which requires different simulation tools, it has been simulated as a port operating at the desired frequency.

The modulator is designed with a length of 6 μm, to provide a phase change of π, or half the wavelength [13]. To correctly record the phase delay produced by the modulator, the electric field at the output of the modulator is measured as the Fermi energy of the graphene layer is changed. Figure 2 shows that for a Fermi energy in the range of 0.15 eV to 0.65 eV the modulator meets this criteria. Figure 2 also shows that for small values of Fermi energy, the SPP waves propagate slower, and thus the power dissipation is greater.

The antenna is designed as exactly in [13], with a resonant length of 9 μm. The S11 parameter (reflection coefficient) of the antenna, which should be less than -10 dB for acceptable performance, is at -21.3 dB at the frequency of interest. This is shown in Fig 3.

The modulator and the antenna are modeled identically. The difference in their performance characteristics arises due to the fact that the antenna has a fixed Fermi energy, which has been

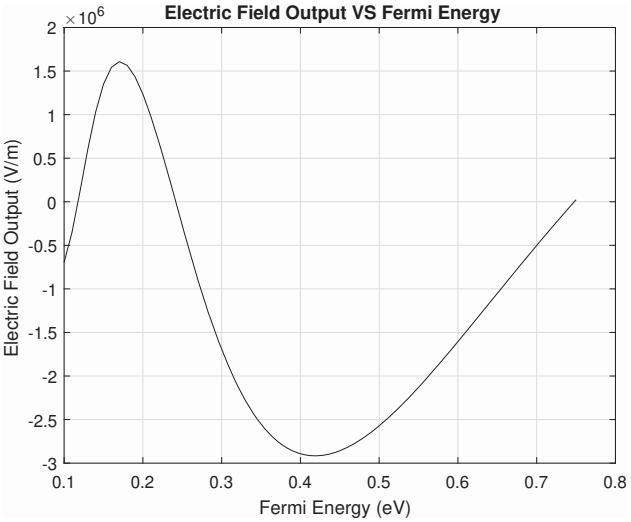

Fig. 2. Electric field output at modulator, showing phase deviation.

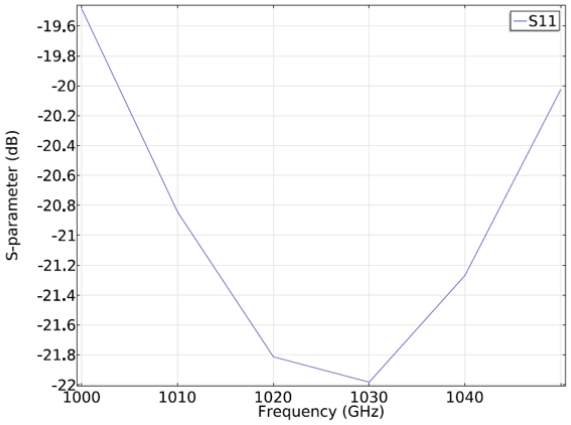

Fig. 3. Reflection coefficient of antenna, reproduced from [13].

selected for resonance at the desired frequency, in line with the antenna's physical dimensions. The modulator on the other hand does not have a fixed Fermi energy, but a variable one. This variation changes the arrival phase of the SPP waves as they are fed into the nano-antenna, and not for expected resonance at any frequency.

However, the modulator still acts as a component in the radiation pattern from the front end, as a "bad antenna". The change in the Fermi energy of the modulator changes the effective impedance of the modulator block. Thus, the effect of the modulator on the overall radiation from the front end is non-trivial.

Figure 4 shows three key elements. Surface 1 represents the antenna, while surface 2 represents the modulator. Line 3 shows the imaginary boundary where the antenna and the modulator are joined, with a variable impedance dependent on the Fermi energy of the modulator.

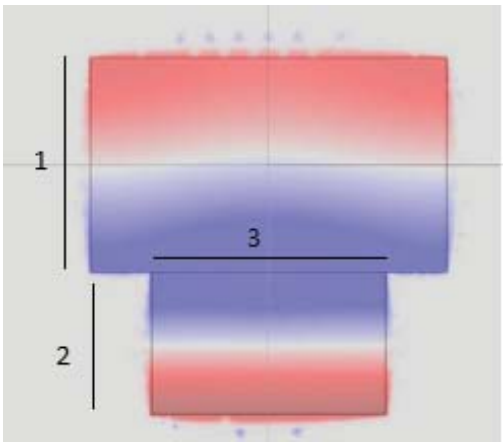

Fig. 4. Joint antenna modulator effect

Due to this varying impedance and the fact that the modulator and the antenna are essentially a continuous chain, the reflection coefficient at the modulator/antenna junction cannot be monitored easily. Only the resulting changes to the radiation pattern can be observed as the Fermi energy of the modulator block is varied. Thus, to perform dynamic beam-forming with the array based on the plasmonic architecture discussed, the combined effect of array factor, as well as the radiation pattern of a single antenna need to be taken into account.

IV. Beamforming

In this section the beamforming capabilites of a single antenna, as well as an array based upon the architecture from the previous sections, are discussed. The results from this section are illustrated in Sec V.

A. Reconfiguration Pattern of a Single Antenna

Most phased arrays consist of broadside or dipole antennas. Usually, the radiation pattern of a single antenna element is fixed and independent of the phase for that element [17]. It is the combined effect of the phases of all the array elements that decide the main beam direction. This phenomenon has been exhaustively researched and studied, and algorithms have been developed for precise beamforming.

Recently, single antennas with reconfigurable radiation patterns have been proposed [18]. These use multi-port antennas, which can be fed from different points thus giving rise to different radiation patterns. The method of feed rotation for antennas can also be used to re-configure the radiation pattern of that particular antenna [19]. These features have been proposed, however, for frequencies well below the THz range. Since each feed point encounters different impedances, as well as different effective antenna dimensions, the radiation pattern is altered [18].

The plasmonic front end also has single antenna beamforming capability. The radiation response depends on both modulator and the nano antenna, and the modulator response varies as per the Fermi energy of graphene. This feature gives our architecture the ability to reconfigure the radiation pattern without altering the feed points, or increasing the design complexity. A single control line for all the modulator blocks can be used to beamform with this advantage. It does however make the calculation of optimal array weights a more complex task.

B. Array

In conventional beamforming an array comprising of antenna elements spaced evenly apart (usually one-half of the free space wavelength) with a precalculated phase difference is used to direct the beam in a main direction. The advantages of this design are that the beam is concentrated in a particular direction towards the receiver, rather than in an omnidirectional pattern. The relative phase difference between the array elements controls the direction of the beam [17]. The relation between phase delay and the broadside angle deviation has been understood in beamforming theory. A phased array can, and will, change the beam direction pattern.

In conventional array design, mutual coupling requires that at least one quarter wavelength of spacing be kept between the array elements [17]. In the case of plasmonic array architecture, mutual coupling does not play a major role since the limiting factor is the plasmonic wavelength and is much lesser than the free space wavelength [14]. Thus, in theory, the antenna elements could be spaced very closely. Since this is a feature that needs to be studied in detail, and keeping computational limitations in mind, the array elements were kept at one-half wavelength distance from each other in the simulated array.

There are two main benefits of beam-forming in our case:

1) Increase in power with every additional element, thus increasing the transmission distance.
2) Control over beam direction, both with single control line as well as multiple control lines.

With multiple antennas, the power output is increased. This advantage, along with the fact that the individual front end footprint in a plasmonic antenna will be signifiacntly smaller than for a regular patch antenna front end, means that even upwards of a 1000 elements could be placed closely together in an array, and achieve a high power output in the order of a few μW.

Beamforming with a single control line offers certain advantages in hardware design. The idea is that to control the Fermi energy of the modulator, a modulating voltage signal must be applied to the modulator as previously discussed in modulator design, and outlined in [9]. If the radiation pattern of the single antenna did not change with the modulator phase, this would require multiple control lines, one for each modulating signal. However, since the change in Fermi energy of the modulator on its own changes the radiation pattern of the single front end, a common control line for all the array elements still results in beam-steering.

The advantage of a single control line is obvious. It reduces the hardware complexity and the effect of coupling from the use of multiple transmission lines. However, beamforming

capability is limited by the changes in the pattern of the single front end, and the range of the Fermi energy considered for the modulator. To fully utilize the power of an array, every phase controlling modulator should have an independent modulating signal. Individual control lines would mean that both the single front end radiation pattern as well as the subsequent phase delay between the radiating elements affect the array performance. This increases the range of the radiation pattern produced. It does however, mean that calculating the optimal weights becomes a non-trivial exercise, and require new algorithm consideration. Thus, a beamforming algorithm for this task is still being developed.

V. Results

The results from the previous section are presented here. As aforementioned, COMSOL multiphysics was used as the simulation platform for these analyses.

A. Single Front End

The radiation pattern of a single front end is shown in Fig 5. The modulator was set with the end Fermi energies, to check the range of reconfiguration in radiation possible. The figure shows radiation pattern for two different Fermi energies of the modulator block: 0.15 eV and 0.65 eV. In the case where the modulator was kept at 0.15 eV, the beam is approximately -30 degrees from broadside. With the Fermi energy kept at 0.65 eV, the beam is approximately +30 degrees from broadside.

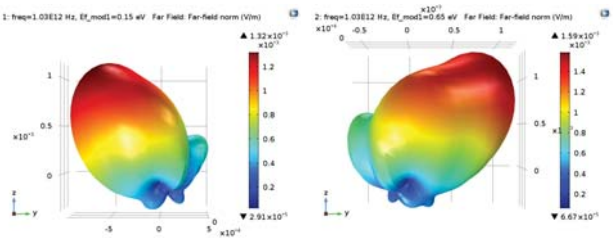

(a) 0.15eV (b) 0.65eV

Fig. 5. The radiation diagram resulting from a single front end, with Fermi energy at a) 0.15 eV and b) 0.65 eV

B. Power Comparison

The effect on the output power of the array as the size of the array is increased is shown in Fig 6. The output power was numerically evaluated up till an array of size 6, and then a polynomial extrapolation was performed.

C. Single Control Line

Figure 7 shows an array with uniform spacing of one-half free space wavelength which was used for array performance analyses. In this case, all the modulators have a Fermi energy of 0.65 eV. As can be seen, strong electric fields are generated across the antenna elements, with all the elements at the same phase. The radiation pattern with a single control line is shown

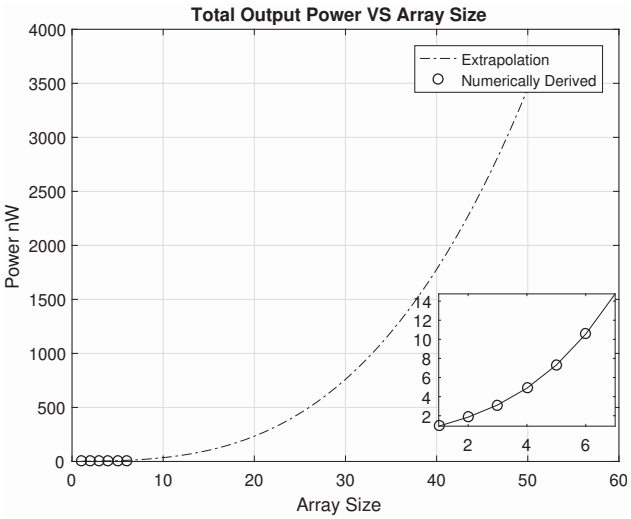

Fig. 6. Output power Vs Array size.

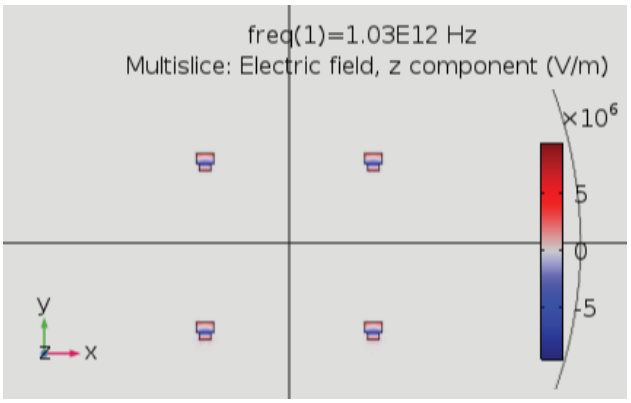

Fig. 7. 2*2 array considered for performance analyses.

in Fig 8. The result is similar to the case with a single front end. However, due to beamforming, the beam is more focused and directional, along with increased power output.

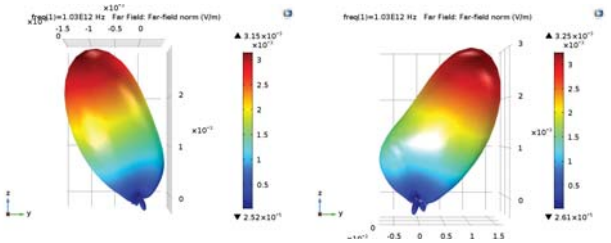

(a) 0.15eV (b) 0.65eV

Fig. 8. The radiation diagram resulting from single control line, with Fermi energy at a) 0.15 eV and b) 0.65 eV

D. Multiple control lines

Table I shows some of the weights used for the modulators of the array and the resulting broadside direction of the beam. The most important thing to note is that the angle of the beam pattern is significantly wider than that possible with a single control line. With a single control line, the radiation pattern is roughly spaced out over 60 degrees across the range of Fermi energy available for the modulator. In the case of multiple control lines, this radiation pattern is extended over a 100 degrees.

TABLE I
ARRAY RADIATION PATTERN WITH MULTIPLE CONTROL LINES

Mod1	Mod2	Mod3	Mod4	Angle Broadside
0.15eV	0.15eV	0.15eV	0.15eV	-30 degrees
0.65eV	0.15eV	0.65eV	0.65eV	+40 degrees
0.65eV	0.4eV	0.15eV	0.65eV	+55 degrees
0.15eV	0.65eV	0.15eV	0.65eV	-45 degrees
0.65eV	0.65eV	0.4eV	0.4eV	+45 degrees
0.4eV	0.4eV	0.4eV	0.4eV	+15 degrees

VI. CONCLUSION AND FUTURE WORK

In this paper, beamforming capabilities were numerically analyzed and investigated for a novel plasmonic architecture based array. The ability to beamform with a single control line was demonstrated, along with the added advantage of individual control. Although these radiating elements can be densely packed together for unprecedented beamforming capabilites, due to computational constraints, a 2x2 array with spacing equal to one-half of the free space wavelength was considered. The advantage in both power output and beam-directivity was shown. The array architecture requires new beamforming algorithm framework which can also be accurately scaled to a densely packed array. The development of this algorithm, with a fully integrated beamforming mechanism, both with phase control as shown in this paper as well as amplitude control, is the focus of future work on this design.

ACKNOWLEDGEMENT OF SUPPORT AND DISCLAIMER

(a) The State University of New York at Buffalo acknowledges the U.S. Government's support in the publication of this paper.

(b) Any opinions, findings and conclusions or recommendations expressed in this material are those of the author(s) and do not necessarily reflect the views of AFRL.

REFERENCES

[1] J. Federici and L. Moeller, "Review of terahertz and subterahertz wireless communications," *Journal of Applied Physics*, vol. 107, no. 11, p. 111101, 2010.

[2] I. F. Akyildiz, J. M. Jornet, and C. Han, "Terahertz band: Next frontier for wireless communications," *Physical Communication (Elsevier) Journal*, vol. 12, pp. 16–32, Sep. 2014.

[3] A. C. Ferrari, F. Bonaccorso, V. Fal'Ko, K. S. Novoselov, S. Roche, P. Bøggild, S. Borini, F. H. Koppens, V. Palermo, N. Pugno *et al.*, "Science and technology roadmap for graphene, related two-dimensional crystals, and hybrid systems," *Nanoscale*, vol. 7, no. 11, pp. 4598–4810, 2015.

[4] L. Falkovsky and S. Pershoguba, "Optical far-infrared properties of a graphene monolayer and multilayer," *Physical Review B*, vol. 76, pp. 1–4, 2007.

[5] V. P. Gusynin and S. G. Sharapov, "Transport of dirac quasiparticles in graphene: hall and optical conductivities," *Physical Review B*, vol. 73, p. 245411, Jun. 2006.

[6] L. Ju, B. Geng, J. Horng, C. Girit, M. martin, Z. Hao, H. Bechtel, X. Liang, A. Zettl, Y. R. Shen, and F. Wang, "Graphene plasmonics for tunable terahertz metamaterials," *Nature Nanotechnology*, vol. 6, pp. 630–634, Sep. 2011.

[7] F. H. L. Koppens, D. E. Chang, and F. J. Garcia de Abajo, "Graphene plasmonics: a platform for strong light matter interactions," *Nano Letters*, vol. 11, no. 8, pp. 3370–3377, Aug. 2011.

[8] J. M. Jornet and I. F. Akyildiz, "Graphene-based plasmonic nano-transceiver for terahertz band communication," in *Proc. of European Conference on Antennas and Propagation (EuCAP)*, 2014.

[9] P. K. Singh, G. Aizin, N. Thawdar, M. Medley, and J. M. Jornet, "Graphene-based plasmonic phase modulator for terahertz-band communication," in *Proc. of the European Conference on Antennas and Propagation (EuCAP)*, 2016.

[10] S. H. Lee, H.-D. Kim, H. J. Choi, B. Kang, Y. R. Cho, and B. Min, "Broadband modulation of terahertz waves with non-resonant graphene meta-devices," *IEEE Transactions on Terahertz Science and Technology*, vol. 3, no. 6, pp. 764–771, 2013.

[11] J. M. Jornet and I. F. Akyildiz, "Graphene-based plasmonic nano-antenna for terahertz band communication in nanonetworks," *IEEE JSAC, Special Issue on Emerging Technologies for Communications*, vol. 12, no. 12, pp. 685–694, Dec. 2013.

[12] J. E. Burke, "Analytical study of tunable bilayered-graphene dipole antenna," Army Armament Research, Development and Engineering Center, Dover, NJ, USA, Tech. Rep., Mar. 2011.

[13] N. Thawdar, J. M. Jornet, and I. Michael Andrello, "Modeling and performance analysis of a reconfigurable plasmonic nano-antenna array architecture for terahertz communications," *NanoCom'18: ACM The Fifth Annual International Conference on Nanoscale Computing and Communication*.

[14] L. Zakrajsek, E. Einarsson, N. Thawdar, M. Medley, and J. M. Jornet, "Design of graphene-based plasmonic nano-antenna arrays in the presence of mutual coupling," in *Proc. of the 11th European Conference on Antennas and Propagation (EuCAP)*, 2017.

[15] W. Knap, J. Lusakowski, T. Parenty, S. Bollaert, A. Cappy, V. Popov, and M. Shur, "Terahertz emission by plasma waves in 60 nm gate high electron mobility transistors," *Applied Physics Letters*, vol. 84, no. 13, pp. 2331–2333, 2004.

[16] T. Otsuji, T. Watanabe, S. Boubanga Tombet, A. Satou, W. Knap, V. Popov, M. Ryzhii, and V. Ryzhii, "Emission and detection of terahertz radiation using two-dimensional electrons in III-V semiconductors and graphene," *IEEE Transactions on Terahertz Science and Technology*, vol. 3, no. 1, pp. 63–71, 2013.

[17] C. A. Balanis, *Antenna Theory: Analysis And Design*. Wiley, 2005.

[18] D. Heberling and C. Oikonomopoulos-Zachos, "Multiport antennas for mimo-systems," in *2009 Loughborough Antennas Propagation Conference*, Nov 2009, pp. 65–70.

[19] J. Costantine, S. Al-Saffar, C. G. Christodoulou, K. Y. Kabalan, and A. El-Hajj, "The analysis of a reconfigurable antenna with a rotating feed using graph models," *IEEE Antennas and Wireless Propagation Letters*, vol. 8, pp. 943–946, 2009.